PERGAMON

Chaos, Solitons and Fractals 12 (2001) 219–234

CHAOS
SOLITONS & FRACTALS

www.elsevier.nl/locate/chaos

A chaotic attractor in ecology: theory and experimental data

J.M. Cushing [a,*], Shandelle M. Henson [b], Robert A. Desharnais [c], Brian Dennis [d], R.F. Costantino [e], Aaron King [f]

[a] *Department of Mathematics, University of Arizona, 617 N. Santa Rita, Tucson, AZ 85721, USA*
[b] *Department of Mathematics, The College of William and Mary, 114 Jones Hall, Williamsburg, VA 23185, USA*
[c] *Department of Biology and Microbiology, California State University, Los Angeles, CA 90032, USA*
[d] *Department of Fish and Wildlife Resources and Division of Statistics, University of Idaho, Moscow, ID 83844, USA*
[e] *Department of Biological Sciences, University of Rhode Island, Kingston, RI 02881, USA*
[f] *Interdisciplinary Program in Applied Mathematics, University of Arizona, 617 N. Santa Rita, Tucson, AZ 85721, USA*

Abstract

Chaos has now been documented in a laboratory population. In controlled laboratory experiments, cultures of flour beetles (*Tribolium castaneum*) undergo bifurcations in their dynamics as demographic parameters are manipulated. These bifurcations, including a specific route to chaos, are predicted by a well-validated deterministic model called the "LPA model". The LPA model is based on the nonlinear interactions among the life cycle stages of the beetle (larva, pupa and adult). A stochastic version of the model accounts for the deviations of data from the deterministic model and provides the means for parameterization and rigorous statistical validation. The chaotic attractor of the deterministic LPA model and the stationary distribution of the stochastic LPA model describe the experimental data in phase space with striking accuracy. In addition, model-predicted temporal patterns on the attractor are observed in the data. This paper gives a brief account of the interdisciplinary effort that obtained these results.

1. Introduction

Erratic fluctuations in population numbers have long fascinated and puzzled ecologists. Prior to the seminal work of Sir R.M. May in the 1970s, the prevailing paradigm viewed such unpredictable fluctuations as random effects due to environmental noise and/or measurement errors. In the absence of noise, according to this view, population numbers would either equilibrate or settle into regular periodic oscillations (induced, for example, by seasonal fluctuations or predator/prey interactions). May's [1,2] writings popularized the now familiar fact that erratic fluctuations can arise from deterministic processes. As Li and Yorke [3] rigorously proved, simple scalar (deterministic) recursion formulas can produce a type of extraordinarily complicated dynamics which they called "chaos". May warned, however, that documenting deterministic chaos in natural population data would not be easy, since it would be difficult to distinguish chaos from noise.

The warning proved prophetic: ecologists have yet to find an unequivocal example of chaos in a natural population [4]. This is not surprising, and the reason is not only the pervasive presence of noise in ecological systems. In fact, the more general problem of connecting nonlinear theory to observed population fluctuations via mathematical models has proved a formidable challenge for both ecologists and mathematicians.

* Corresponding author. Fax: +1-520-621-8322.
E-mail address: cushing@math.arizona.edu (J.M. Cushing).

0960-0779/00/$ - see front matter
PII: S0960-0779(00)00109-0

The successful use of mathematical models is commonplace in other disciplines, and confidence in their ability to describe and predict runs high (indeed, this is to a large extent why certain sciences are called "hard"). In ecology, however, while they have been phenomenologically and qualitatively successful, mathematical models have been considerably less successful with regard to quantitative descriptions and predictions. There are many reasons for this [5,6]. Not only is noise ubiquitous, but fundamental "laws" are scarce, data time series are short, replicate data series are difficult to obtain, manipulations are impractical, parameters cannot be controlled, statistical methodologies are inadequate, and so on. In view of this situation, conclusions asserting specific dynamic properties of a data set – especially a complicated property such as chaos – are rightly viewed with skepticism by ecologists.

The complexity of natural systems, together with the inherent difficulties in confidently linking such systems with theory, points to the need for controlled laboratory experiments – experiments designed and analyzed for the purpose of testing the predictions of nonlinear population theory. Our research team initiated such a project in the early 1990s, using species of flour beetles (genus *Tribolium*) as the experimental animal. Although laboratory microcosms are no substitute for field experiments, they are useful for testing basic ecological hypotheses in isolation from confounding factors. The *Tribolium* system features accurate census counts, long data sets (over many generations), the minimization of noise, and a life-cycle with identifiable stages and interesting nonlinear feedbacks. Because we can manipulate demographic parameters in flour beetle populations we have been able to focus on the rigorous testing of mathematical models.

A major goal of our project is to document the occurrence of a variety of nonlinear phenomena in population dynamics. This includes a spectrum of asymptotic attractors (ranging from equilibria to cycles to chaos) and their bifurcations [7–11], transient phenomena (e.g., the influence of unstable invariant sets) [12,13], multiple attractors and their basins of attraction [13,14], resonances in periodically forced habitats [15,16], and many others. One highlight of the project is the documentation of chaotic dynamics in an ecological population.

2. Modeling methodology

What are the components necessary for a convincing mathematical model in ecology? A modeling exercise in population biology should contain at least the following basic ingredients [5,6]:

First, the model should not be ad hoc, but instead should be based on specific mechanisms judged important by biologists with regard to the dynamics of the population. There is, of course, a tradeoff between detail and tractability. A model with too many variables relative to the amount of data available is not statistically testable. By identifying and isolating dominant mechanisms one can hope to build a model with an appropriately small number of parameters and state variables.

Second, since noise is ubiquitous in biological data, a stochastic version of the model must be constructed in order to account for inevitable deviations from the predictions of the deterministic model [7]. The manner in which the noise is modeled should be based on biological considerations. The stochastic model becomes a statistically testable hypothesis for the explanation of data [7] and therefore provides the means for a strong connection between model and data.

Third, parameter estimation and model validation from data should be distinct procedures. Some model parameters can be estimated independently; others might be experimentally controlled. Inevitably, others must be statistically estimated (with confidence intervals) from data by some method, e.g., maximum likelihood or conditional least squares methods. It is crucial that the data used for parameter estimation not be used to evaluate the accuracy of the model. Otherwise, in a sense, the model cannot go wrong, since by design it "fits" or "interpolates" the data in some optimal manner; and a model that cannot fail provides little information.

Fourth, a good model is predictive as well as descriptive. Indeed, the strongest case for a model is made when it provides predictions which subsequently can be documented by observations or controlled experiments and rigorous statistical analyses.

More details regarding our methodology appear in [6,7].

For nearly a decade we have collaborated on interdisciplinary projects in which these modeling principles are applied to the investigation of nonlinear phenomena in population biology, using laboratory cultures of flour beetles. As mentioned above, it is a goal of the project to document the occurrence of a variety of nonlinear phenomena in population dynamics, including chaos. However, an equally important goal of the project is to demonstrate that mathematical models can "work" in population dynamics, i.e., that models can provide quantitatively accurate explanations for patterns in data and can provide predictions that we are able to document by carefully controlled and replicated experiments.

3. The LPA models

The dominant mechanisms driving the dynamics of *Tribolium castaneum* (our experimental animal) are cannibalistic interactions among life cycle stages [17]. Specifically, mobile stages (adults and larvae) consume immobile stages (eggs and pupae). For this reason, we utilize a "stage-structured" population model, i.e., a model in which individuals of the population are categorized according to their stage of development: larvae, pupae and adults. The beetles are maintained in 237 ml (1/2 pint) milk bottles with 20 g of standard medium (refreshed at each census) and kept in a dark incubator at 32°C. Each stage is counted at 2-week intervals (which is roughly the length of both the larval and pupal periods under laboratory conditions). Since the egg stage is relatively short (3–5 days), we ignore this stage in the model.

Let L_t, P_t and A_t denote the number of larvae, pupae and adults at time t, respectively. We require formulas for the numbers L_{t+1}, P_{t+1} and A_{t+1}. The unit of time is 2 weeks. If $b > 0$ denotes the larval recruitment rate (per adult per unit time) in the absence of egg cannibalism, then $L_{t+1} = bA_t$. Cannibalistic encounters occur randomly. A probabilistic argument implies that the probability an egg escapes cannibalism in the presence of A adults during a unit of time is $e^{-c_{ea}A}$, where $c_{ea} > 0$ is the adult/egg cannibalism coefficient. Similarly, the probability an egg escapes cannibalism in the presence of L larvae is $e^{-c_{el}L}$, where $c_{el} > 0$ is the larvae/egg cannibalism coefficient. Thus

$$L_{t+1} = bA_t e^{-c_{ea}A_t - c_{el}L_t}.$$

This equation reflects the fact that the larval period is 2 weeks (i.e., none of the larvae present at time t are present at time $t + 1$).

Larvae are not subject to cannibalism. If μ_l is the probability that a larva dies in one unit of time, then

$$P_{t+1} = (1 - \mu_l)L_t.$$

This equation reflects the fact that the pupal period is two weeks (i.e., none of the pupae present at time t are present at time $t + 1$).

Finally, pupae are subject to cannibalism by adults. (Larvae sometimes kill pupae, but we ignore this interaction which is rare relative to other forms of cannibalism.) Virtually all pupae that survive cannibalism by adults emerge as adults in one unit of time. Thus

$$A_{t+1} = P_t e^{-c_{pa}A_t} + (1 - \mu_a)A_t,$$

where μ_a is the probability that an adult dies in one unit of time and $c_{pa} > 0$ is the *adult/pupae cannibalism coefficient*.

To summarize, the model equations are:

$$\begin{aligned} L_{t+1} &= bA_t e^{-c_{ea}A_t - c_{el}L_t}, \\ P_{t+1} &= (1 - \mu_l)L_t, \\ A_{t+1} &= P_t e^{-c_{pa}A_t} + (1 - \mu_a)A_t \end{aligned} \tag{1}$$

for $t = 0, 1, 2, \ldots$ This system of recursion (or "difference") equations has the form of a nonlinear Leslie matrix model [18]. The equations define a discrete semi-dynamical system.

The Ricker equation $x_{t+1} = bx_t e^{-cx_t}$ appears frequently in the literature as a dynamic model for a population with non-overlapping generations. The LPA model described by Eqs. (1) is an extension of the

Ricker model to a case of overlapping generations. The Ricker equation displays the famous period doubling route to chaos (similar to the familiar, but less biologically relevant discrete logistic equation $x_{t+1} = bx_t(1 - cx_t)$). Thus, we can expect the LPA model (1) to exhibit complex dynamics, including a route to chaos, although not necessarily a period doubling route.

Basic facts about the dynamics of the LPA model can be found in [18]. The positive cone R_3^+ is forward invariant and (1) is point dissipative. Specifically, there is a box $0 \leqslant L \leqslant L^*$, $0 \leqslant P \leqslant P^*$, $0 \leqslant A \leqslant A^*$ inside of which all orbits starting in R_3^+ remain after a finite number of time steps. This implies there exists a global, connected attractor in the box [19]. For $b < \mu_a/(1 - \mu_l)$ the global attractor is the equilibrium $(L, P, A) = (0, 0, 0)$, i.e., all orbits starting in R_3^+ tend to $(0, 0, 0)$ as $t \to +\infty$ and the population goes extinct. For $b > \mu_a/(1 - \mu_l)$ the origin is unstable and (1) is uniformly persistent (permanent) with respect to the origin $(L, P, A) = (0, 0, 0)$. That is, there exists an $\epsilon > 0$ such that $\liminf_{t\to+\infty}(L(t) + P(t) + A(t)) \geqslant \epsilon$ for all non-negative initial conditions $(L(0), P(0), A(0)) \neq (0, 0, 0)$. Also, for $b > \mu_a/(1 - \mu_l)$ there exists a unique, positive equilibrium. This equilibrium is locally asymptotically stable for b sufficiently close to $\mu_a/(1 - \mu_l)$. For other values of the parameters the equilibrium may, however, be unstable and bifurcations to either 2-cycles or to aperiodic, invariant loops may occur. For example, Fig. 1 illustrates a 2-cycle bifurcation as the adult death rate μ_a is increased through approximately 0.1 and a reverse 2-cycle bifurcation and re-equilibration as μ_a is increased through approximately 0.6. Also seen in Fig. 1 is an invariant loop bifurcation (sometimes called a discrete Hopf or Naimark/Sacker bifurcation) at approximately $\mu_a = 0.95$. Changes in other parameters may lead to different bifurcations, including those giving rise to chaotic and strange attractors.

To account for deviations of data from the deterministic predictions of the LPA model (1) we construct a stochastic version of the model in which a specific kind of noise is introduced. The resulting stochastic LPA model serves to connect the *deterministic skeleton* [20] defined by (1) with data; it provides the means to estimate parameters, construct confidence intervals for these estimates, and statistically test the accuracy of the model [7,11].

Ecologists distinguish two general types of noise in ecological systems: demographic and environmental stochasticity [21,22]. Roughly speaking, demographic random events act at the individual level (e.g., an individual survives one unit of time with a certain probability) while environmental random events act at an aggregate population level (e.g., the per capita birth or death rates for all adults randomly change). Demographic noise may be expected to play the most important role when population numbers are low, whereas environmental noise is expected to be more important when population numbers are high. Either type of noise (indeed, a weighted mixture of both types) can be modeled by a nonlinear autoregressive process of the form

$$X_{t+1} = f(X_t) + E_t,$$

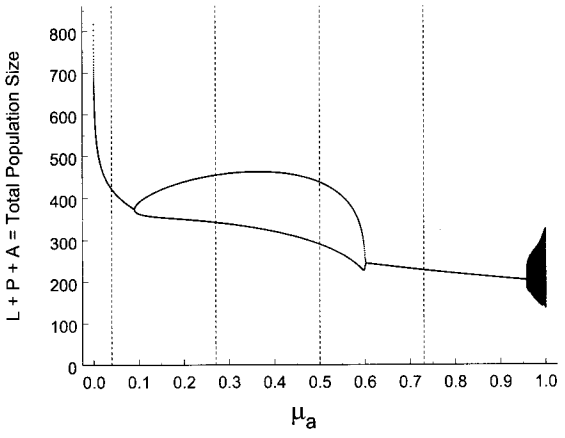

Fig. 1. A bifurcation diagram is shown for the deterministic LPA model (1) using the parameter μ_a. The other model parameter values are $b = 7.483$, $\mu_l = 0.2670$, $c_{ea} = 0.009170$, $c_{el} = 0.01200$, $c_{pa} = 0.004139$. The vertical dashed lines indicate those μ_a values at which laboratory experiments were performed [8,9].

where X_t is a vector of suitably transformed [1] state variables and E_t is a vector of normal random variables with mean 0. This formulation has the major advantage of bringing to bear a full suite of statistical inference methods for time series analysis [7,9,20]. In the case of environmental noise a logarithmic transformation is appropriate, whereas for demographic noise a square root transformation is appropriate.

For example, the demographic noise LPA model is described by the equations:

$$\begin{aligned} L_{t+1} &= \left\lfloor \sqrt{bA_t \mathrm{e}^{-c_{\mathrm{ea}}A_t - c_{\mathrm{el}}L_t}} + E_{1t} \right\rfloor^2, \\ P_{t+1} &= \left\lfloor \sqrt{(1-\mu_{\mathrm{l}})L_t} + E_{2t} \right\rfloor^2, \\ A_{t+1} &= \left\lfloor \sqrt{P_t \mathrm{e}^{-c_{\mathrm{pa}}A_t} + (1-\mu_{\mathrm{a}})A_t} + E_{3t} \right\rfloor^2, \end{aligned} \tag{2}$$

where $\lfloor x \rfloor = \max\{0, x\}$ and the environmental noise LPA model is described by the equations:

$$\begin{aligned} L_{t+1} &= bA_t \mathrm{e}^{-c_{\mathrm{ea}}A_t - c_{\mathrm{el}}L_t} \mathrm{e}^{E_{1t}}, \\ P_{t+1} &= (1-\mu_{\mathrm{l}})L_t \mathrm{e}^{E_{2t}}, \\ A_{t+1} &= \left(P_t \mathrm{e}^{-c_{\mathrm{pa}}A_t} + (1-\mu_{\mathrm{a}})A_t\right) \mathrm{e}^{E_{3t}}. \end{aligned} \tag{3}$$

Here $E_t = (E_{1t}, E_{2t}, E_{3t})$ is a random noise vector assumed to have a joint probability distribution with a mean vector of zeros and a (symmetric) variance–covariance matrix denoted by $\Sigma = (\sigma_{ij})$. The noise variables are assumed uncorrelated through time. The deterministic LPA model (1) is obtained by setting $(E_{1t}, E_{2t}, E_{3t}) = (0,0,0)$, or equivalently $\Sigma = 0$.

The stochastic models (2) and (3) are the cornerstones of our project. They contain both the relevant deterministic forces and a statistical description of the stochastic deviations from the deterministic skeleton (1). As such they constitute testable hypotheses to be confronted with data. The next step is to parameterize and validate these models.

4. Model parameterization and validation

In [7] we parameterized the LPA model (1) using a historical data set by means of both maximum likelihood and conditional least squares methods. (Estimates for the entries in Σ also were obtained.) In addition, a variety of statistical validation tests are described in [7], as are the results of applying these tests to the LPA model. On the basis of this validation, we used the model and the estimated parameters to design a (first) laboratory experiment. The purpose of this experiment was to document the bifurcations predicted by the model as a parameter is changed. Specifically, using the bifurcation diagram in Fig. 1 as a guide, we manipulated the adult death rates μ_{a} of several laboratory cultures of *T. castaneum*. For each selected value of μ_{a} the treatment was replicated three times (as was an unmanipulated control culture). The results are reported in [8]. Detailed statistical analyses of the model and the data (as well as a description of the experiment) appear in [9]. Fig. 2 illustrates graphically the results of this experiment and shows visually how well the model correctly predicted the attractor. (An experiment using a different genetic strain of *T. castaneum* also proved successful.)

Bolstered by the descriptive and predictive success of the LPA model in the first experiment, we designed a second experiment involving a more complicated sequence of bifurcations, a sequence that includes chaotic (and strange) attractors (see Fig. 3). The experiment involves the manipulation of both model parameters μ_{a} and c_{pa}. [2] The death rate is held constant at $\mu_{\mathrm{a}} = 0.96$ while c_{pa} is assigned a selection of values from 0 to 1 as indicated in Fig. 3. The results after 80 weeks were announced in [10]. Using the resulting data, we examined both the demographic and environmental noise models (2) and (3). We

[1] The transformation is chosen so as to stabilize the variability of the process.

[2] At each census time all live and dead adults are counted. This allows for a manipulation of both the adult death rate and recruitment rate.

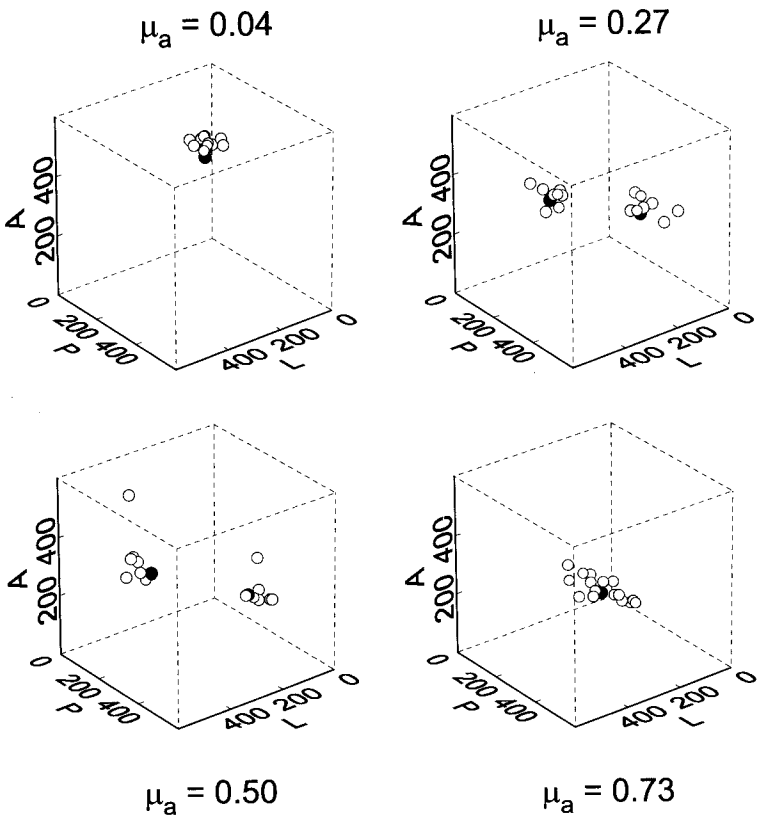

Fig. 2. The open circles are (L,P,A) data points, with transients removed, obtained from experiments at the c_{pa} values indicated in Fig. 1. The solid circles indicate the predicted attractors of the deterministic LPA model (1), as seen in Fig. 1.

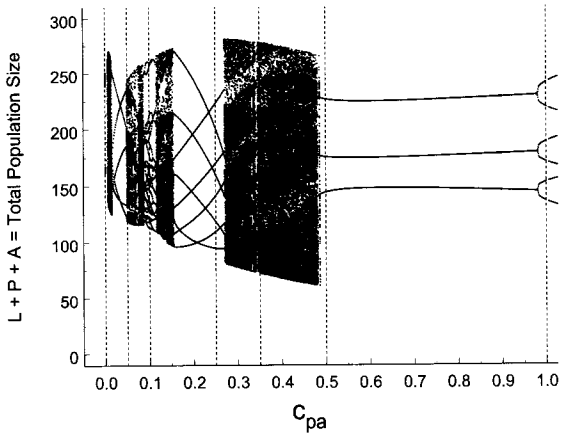

Fig. 3. A bifurcation diagram is shown for the deterministic LPA model (1) using the parameter c_{pa}. Other parameter values are those appearing in Table 1, together with $\mu_a = 0.96$. The vertical dashed lines indicate those c_{pa} values at which laboratory experiments were performed [10,11].

estimated parameters, using a conditional least squares procedure, and conducted diagnostic analyses using a variety of statistical tests (including homoskedasticity, autocorrelations, normality of residuals, fitted R^2 values, and normal quantile–quantile plots). These analyses show that the deterministic skeleton (1) does an outstanding job of describing the experimental data. For example, on average the model accounts for 90%

Table 1
Parameter estimates for the deterministic LPA (1) model were obtained using data from an experiment in which c_{pa} was held fixed and $\mu_a = 0.96$ [a]

Parameter	CLS estimate	95% Confidence interval
b	10.45	(10.04, 10.77)
μ_l	0.2000	(0.1931, 0.2068)
c_{el}	0.01731	(0.01611, 0.01759)
c_{ea}	0.01310	(0.01285, 0.01340)

[a] Estimates for the entries in the variance–covariance matrix Σ for the demographic stochastic model (2) are $\sigma_{11} = 2.332$, $\sigma_{22} = 0.2374$, $\sigma_{12} = \sigma_{21} = 0.007097$. For this experiment Σ is a 2×2 matrix since, by the experimental design, the third equation in (1) is exact and hence $E_{3t} = 0$ for all t.

of the variability in the L-stage and 99% of the variability in the P-stage across all treatments. [3] The analyses also show that the demographic noise model (2) better describes the experimental data than does the environmental noise model (3). Confidence intervals for the parameter estimates were computed using a bootstrapping technique. The results (based on the demographic noise model (2)) appear in Table 1. A full report of these analyses appears in [11].

From the bifurcation diagram in Fig. 3 we see a variety of attractors are predicted by the deterministic model (1) for the selected c_{pa} values. A complete discussion of the results at each c_{pa} value appears in [11]. Fig. 4 illustrates the results of the experiment in the two cases $c_{pa} = 0.00$ and 1.00. The graphs compare experimental data, deterministic attractors of (1), and the stationary distributions of (2). Fig. 4 illustrates graphically how well the demographic noise model predicts the long term dynamics of the beetles and how much the deterministic attractor influences those dynamics. Furthermore, the experimental data plotted in Fig. 4 clearly corroborates the model predicted transitions, both deterministic and stochastic, as c_{pa} is changed from 0.00 to 1.00.

A complicated array of bifurcations and attractors occurs for values of c_{pa} between 0.00 to 1.00 (Fig. 3), including, as we shall see in the next section, chaotic attractors.

5. The chaotic attractor

The deterministic LPA model (1) has a global, chaotic attractor when $c_{pa} = 0.35$ (with $\mu_a = 0.96$ and the parameter values listed in Table 1). The dominant Lyapunov exponent of the attractor [23] is 0.0959 with a 95% confidence interval of $(-0.066, 0.100)$, [4] and a non-integer "fractal" Lyapunov dimension [23] of 1.26. We now focus our attention on this attractor and the data from this treatment of the experiment. We note chaos is robust throughout the parameter confidence intervals in Table 1; see Fig. 5 (also see [11]).

The positive LE indicates that, on an average, the attractor has sensitivity to initial conditions, a hallmark of chaos. A graph of the chaotic attractor, color coded to show sensitivity to initial conditions at each point, appears in Fig. 6. The "hot spot", where orbits exponentially diverge at the greatest rate (colored red), occurs when pupal numbers are high and adult and larval numbers are both low. Sensitivity to initial conditions can also be measured for the stochastic LPA model (2) by using the stochastic Lyapunov exponent (SLE) [24]. The SLE is calculated by averaging over the stationary distribution for the stochastic model (2), while the LE is averaged over the attractor of the deterministic model (1). Using the estimates for the variance–covariance matrix Σ in Table 1, we calculated the SLE of (2) to be 0.053, with a 95% confidence interval of $(0.049, 0.055)$. A color-coded representation of the stationary distribution is illustrated in Fig. 7. This is the predicted distribution of data points for the $c_{pa} = 0.35$ treatment of the experiment.

[3] The A-stage is effectively deterministic due to the experimental protocol of controlling μ_a and c_{pa}.
[4] The remaining two Lyapunov exponents are -0.370 and -6.00.

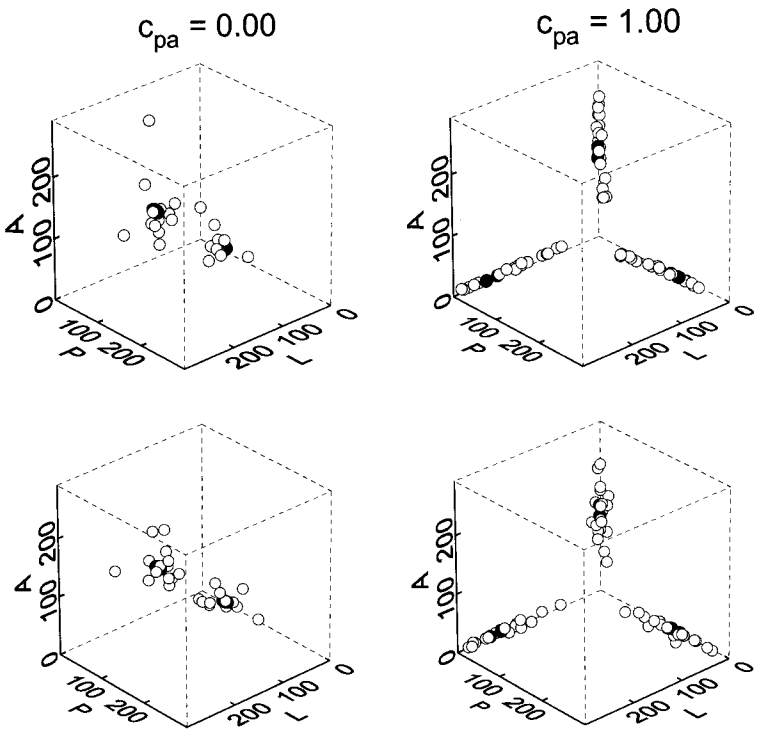

Fig. 4. The upper graphs show the attractor predicted by the deterministic LPA model (1) together with experimental flour beetle data (open circles) for two treatments of the experiment, $c_{pa} = 0.00$ and $c_{pa} = 1.00$. Transients have been removed. For the treatment $c_{pa} = 1.00$ data is shown for weeks 40–80. The model predicts longer transients for the treatment $c_{pa} = 0.00$ and data is shown for weeks 64–80. For purposes of comparison, the same number of points from the stationary distribution of the demographic noise LPA model (2) is shown in the lower graphs. The attractor for the treatment $c_{pa} = 0.00$ appears as two points (and hence as a 2-cycle), but in actuality consists of two very small invariant loops. The attractor for the treatment $c_{pa} = 1.00$ is a 6-cycle which consists of three groups of two nearby points. In both cases note the similarity between the experimental data (upper graphs) and the predicted data points of the demographic noise model (lower graphs), and how closely both are related to the predicted deterministic attractor.

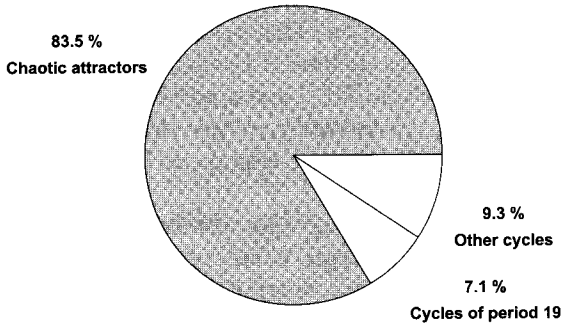

Fig. 5. A pie chart showing the frequency of predicted deterministic attractors at the treatment $c_{pa} = 0.35$ for the 2000 bootstrap parameter estimates (see Fig. 3).

The three replicate cultures grown at $c_{pa} = 0.35$ have been continued and are (at the time of writing) over 240 weeks old. In order to obtain even more data for this treatment, we initiated six new replicates at 80 weeks. These data are plotted in Fig. 8 (with transients during the first 20 weeks removed).

The remarkable accuracy of the model predictions, as quantified by the analyses in [11], is visually apparent in Figs. 7 and 8 where the distribution of experimental data points in phase space is virtually indistinguishable from the stationary distribution predicted by the demographic noise model (2). When the experiment is finally terminated, we will conduct comparison studies of these distributions as further tests of model accuracy.

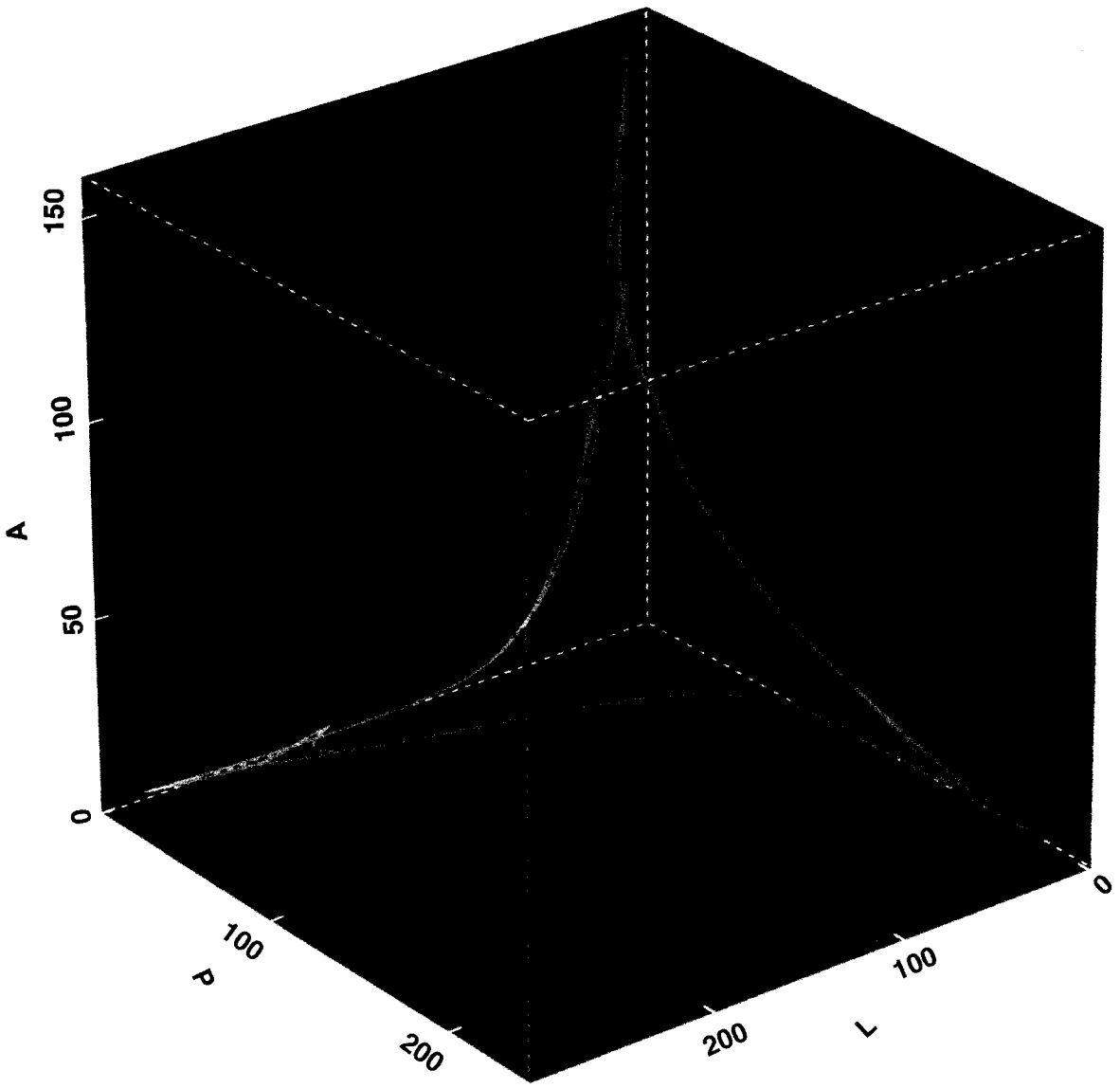

Fig. 6. The chaotic attractor for the deterministic LPA model (1) with $\mu_a = 0.96$, $c_{pa} = 0.35$ and other parameters given in Table 1. This "tangled triangle" attractor is color-coded using the log magnitude of the largest eigenvalue of the Jacobian matrix (the "one-step local Lyapunov exponent"), which ranges from -1.031 (yellow) to 3.9520 (red).

Although the predicted dynamics on the deterministic attractor are chaotic, there are distinctive temporal patterns in the time series. These patterns are predictions of the deterministic model and corroboration can be sought in the experimental data. At $c_{pa} = 0.35$, there exists an unstable saddle cycle of period 11 on the chaotic attractor (Fig. 9). The source of this cycle is an Arnol'd tongue of 11-cycles, with rotation number 4:11, emanating from the curve of invariant loop bifurcation points in the (μ_a, c_{pa}) parameter plane [25] (Fig. 10). Note that this 11-cycle exhibits oscillatory patterns of shorter lengths. For example, in Fig. 9 a plot of the L component of the 11-cycle shows four peaks per period and a distinctive sub-pattern of length 3 (a high-low-low pattern). These patterns are also observed in the model time series of chaotic orbits on the attractor. For example, in Fig. 11 we observe a frequently occurring pattern of length 11 (with four peaks) in the time series of the L component of such an orbit – a pattern that is remarkably similar to that of the saddle 11-cycle. Moreover, this pattern occasionally appears in successive repetitions that form episodes of near periodicity.

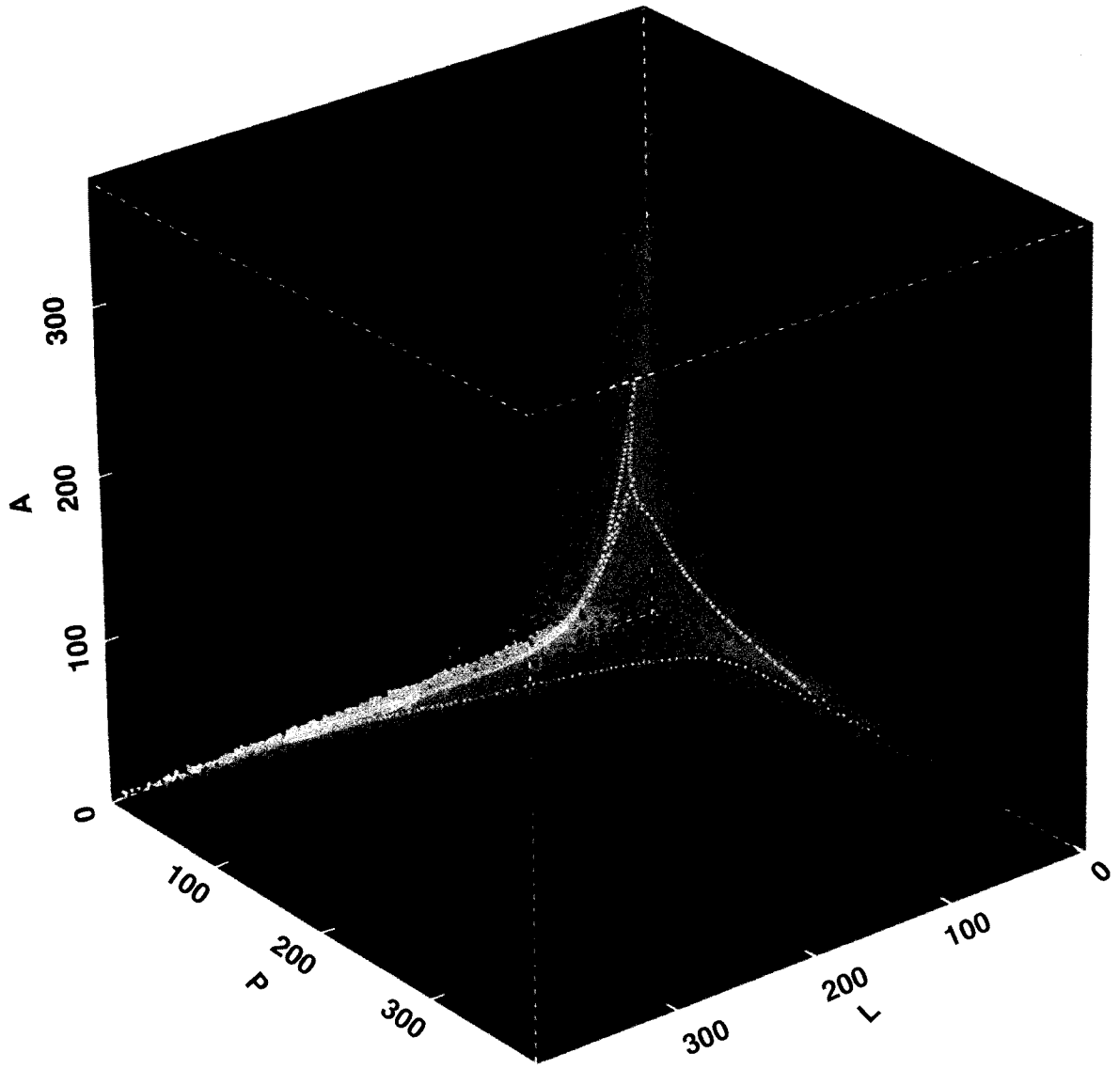

Fig. 7. 7500 points are shown from the stationary distribution of the demographic noise model (2) with parameters from Table 1 and $\mu_a = 0.96$, $c_{pa} = 0.35$. Also shown is the chaotic attractor of the deterministic skeleton (see Fig. 6). The points are color-coded using the log magnitude of the largest eigenvalue of the Jacobian matrix at the point (the "one-step local Lyapunov exponent"), which ranges from -2.742 (yellow) to 4.723 (red).

That the saddle 11-cycle has a dominant influence on the dynamics of the chaotic attractor [25] is also evidenced by the similarity between the power spectrum of the L component of the 11-cycle and that of the attractor shown in Figs. 9 and 12A, both of which show dominant peaks at the base period $11/4 = 2.75$. Power spectra of the L component of orbits obtained from the demographic noise model (2) indicate this base period, and hence the sub-pattern of length 3, survives the demographic noise (as parameterized in Table 1); see Fig. 12B. This model prediction is borne out by the experimental data, which exhibits a distinctive sub-pattern of length 3; see Fig. 12C. However, the larval four-peak pattern, and hence the 11-cycle pattern, are considerably blurred by the noise in both the demographic noise model and the data. At the conclusion of the experiment we will thoroughly study these (and other) model predicted patterns and analyze their occurrence in the data as part of the further documentation of the LPA model's accuracy.

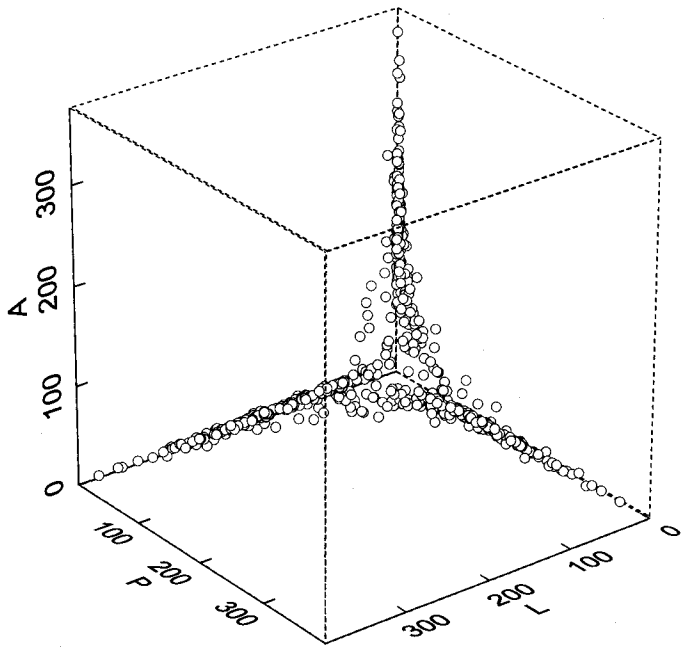

Fig. 8. Data from all replicates of the $c_{pa} = 0.35$ treatment are shown with transients removed.

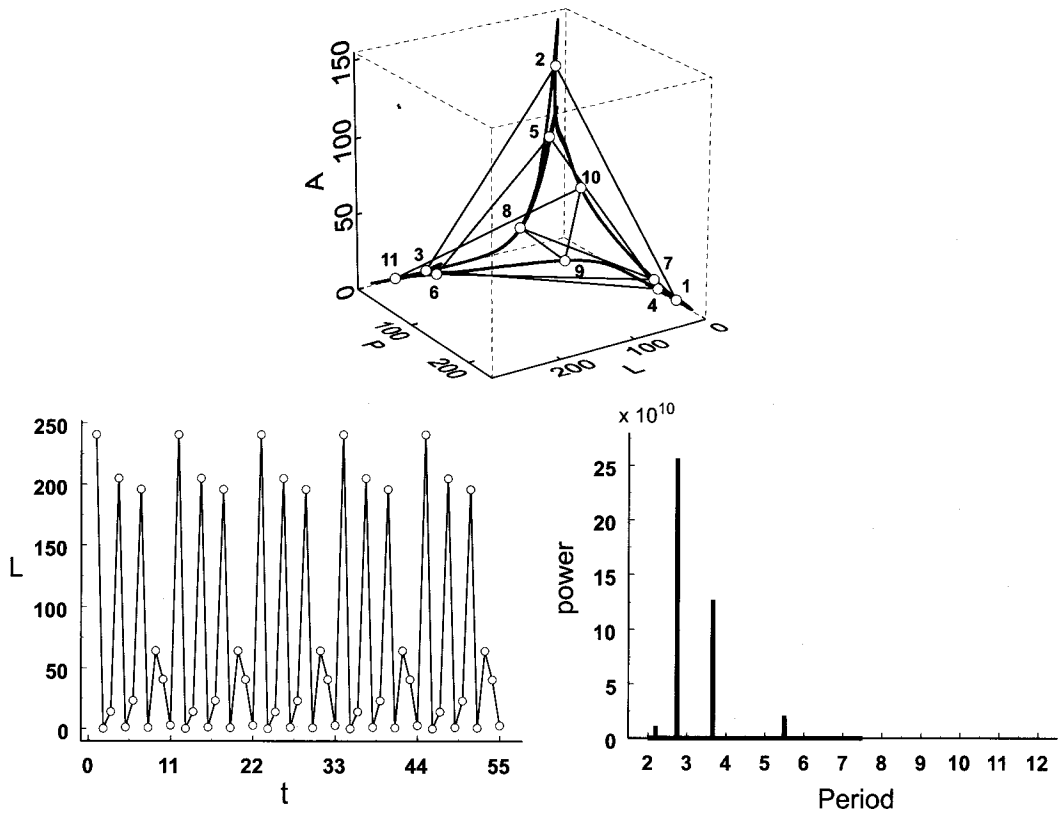

Fig. 9. An unstable 11-cycle on the chaotic attractor in Fig. 6 is shown. Also shown is the L component time series and its power spectrum.

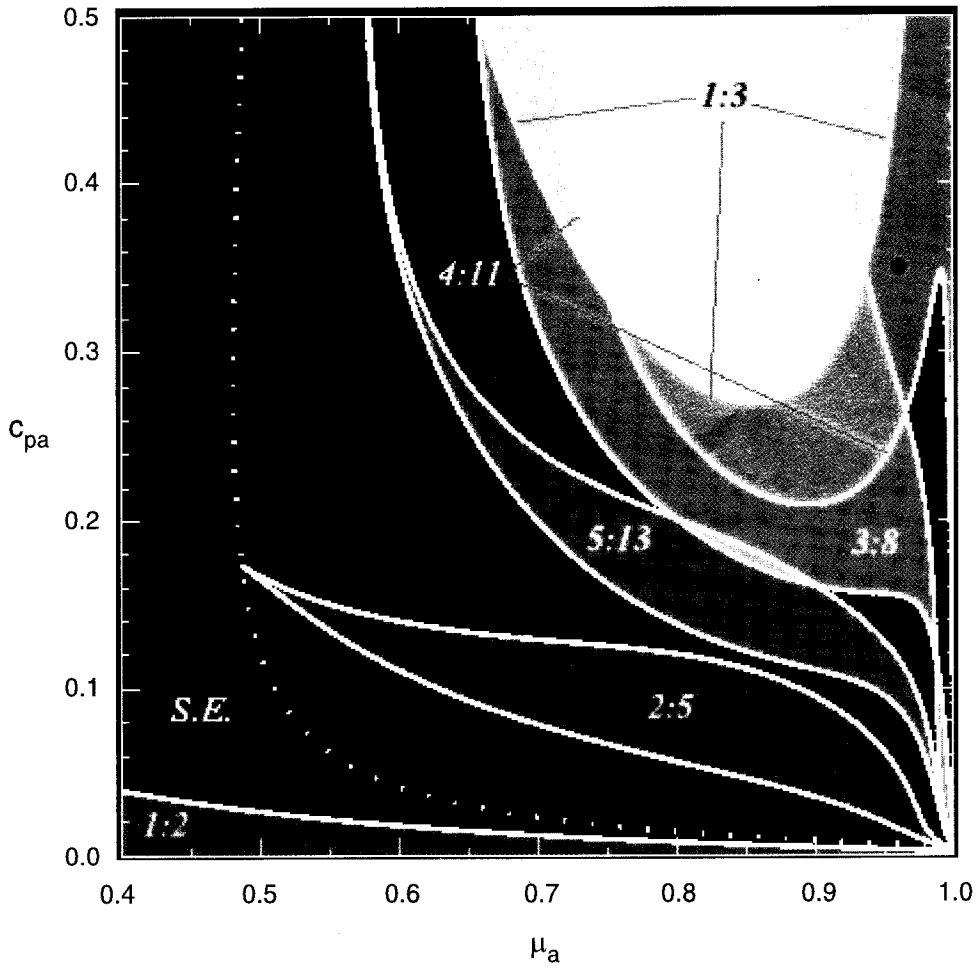

Fig. 10. Selected Arnol'd tongues and their rotation numbers are shown in the (μ_a, c_{pa})-plane for the LPA model (1) with parameters given in Table 1. Globally stable, positive equilibria occur in the region marked S.E. Invariant loop bifurcations occur when the boundary of the S. E. region denoted by the dotted line is crossed. Period doubling bifurcations to a 2-cycle occur when leaving the SE region along the common boundary with the region marked 1:2. The experimental treatment with $\mu_a = 0.96$ and $c_{pa} = 0.35$ (denoted by the black dot) lies in the tongue of 11-cycles with rotation number 4:1.

6. Discussion

The argument that the beetle populations in our experimental treatment at $c_{pa} = 0.35$ are chaotic is based on the accuracy of the LPA model (1). Our confidence in this model is supported by a variety of successful validations. Foremost are the many statistical tests we have performed using data from several experiments, in addition to the bifurcation/chaos experiments described above. We have used the LPA model to provide previously unavailable explanations for observed patterns in data or suggested patterns previously unobserved, including temporal and phase space patterns caused by stable manifolds of unstable saddles [6,12], phase switching in oscillating populations [13], and unexpected resonances due to periodic habitats [15,16]. Also supporting the model's accuracy is its ability to predict, a priori, dynamic patterns subsequently observed in laboratory experiments, such as the bifurcations and attractor patterns in the experiments described above. For other examples of the a priori predictive capability of the model, see [14,26].

Our studies comparing model predicted dynamics with data, whether they deal with exotic dynamics such as chaos or other seemingly less important dynamic patterns, serve at least two important purposes. First, they add to the catalog of nonlinear phenomena rigorously documented to occur in a biological

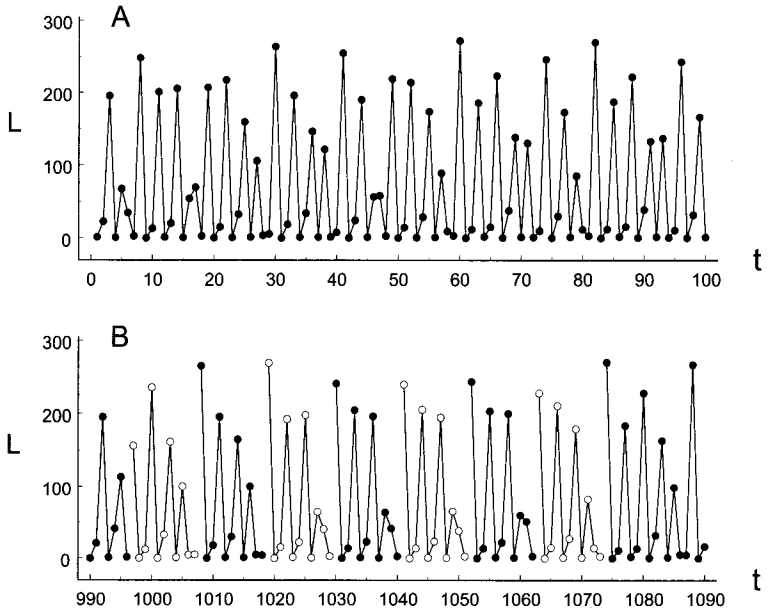

Fig. 11. In graph (A) the L component of a portion of a 10,000-point orbit on the chaotic attractor of the deterministic model (1) shows frequent patterns similar to those of the saddle 11-cycle in Fig. 9. In graph (B) is seen a portion of the orbit during which the pattern is repeated many times in sequence.

population, and by doing so they demonstrate the importance of nonlinear dynamics in ecology. Second, as they accumulate, these studies provide stronger and stronger support for the validity of the LPA model (1) and therefore to biological conclusions based on that model.

For example, we recently implemented another experiment designed to further document the accuracy of model (1), and the properties of its predicted chaotic attractor, in describing the dynamics of flour beetles in the treatment at $c_{pa} = 0.35$. The experimental design is based on a specific characteristic of the chaotic attractor. As the color coding in Figs. 6 and 7 indicates, the region of the attractor most sensitive to initial conditions consists of points with a moderate number L of larvae (say, $L \leqslant 150$) and very low number A of adults (say, $A \leqslant 3$). Numerical explorations using (1) revealed an unexpected consequence of the existence of this "hot" region of the attractor. If, whenever an orbit enters this region, a small perturbation is applied, the resulting long term dynamics are changed in significant ways. Specifically, if only three adults are added each time the orbit enters the hot region, then the number of larvae is decreased, on an average, over 50% and the peak amplitudes of larval numbers are reduced nearly 70%. A similar prediction is also made if the perturbation rule is applied to orbits of the stochastic model (2). Data for the first 26 weeks of the ongoing experiment indicate the model prediction is indeed accurate: small perturbations in adult numbers have a large impact on population abundance.

7. Concluding remarks

Well-validated models such as the deterministic LPA model (1) are rare in population biology. The LPA model therefore provides an unparalleled opportunity to explore and to rigorously document nonlinear phenomena in ecology, at least in a laboratory setting. Nonetheless, noise pervades ecological data and is significant even in our highly controlled experiments. Since no model can capture all mechanisms affecting a population, data inevitably deviates from deterministic model predictions, even in the absence of census errors. It is therefore necessary to account for noise with a stochastic model such as (2) or (3). Unfortunately, the use of stochastic models raises questions concerning the meaningfulness of deterministic concepts such as chaos, or for that matter even equilibria or periodic cycles. Stochastic models do not have deterministic attractors; they have stationary distributions which generally predict that a large portion, if

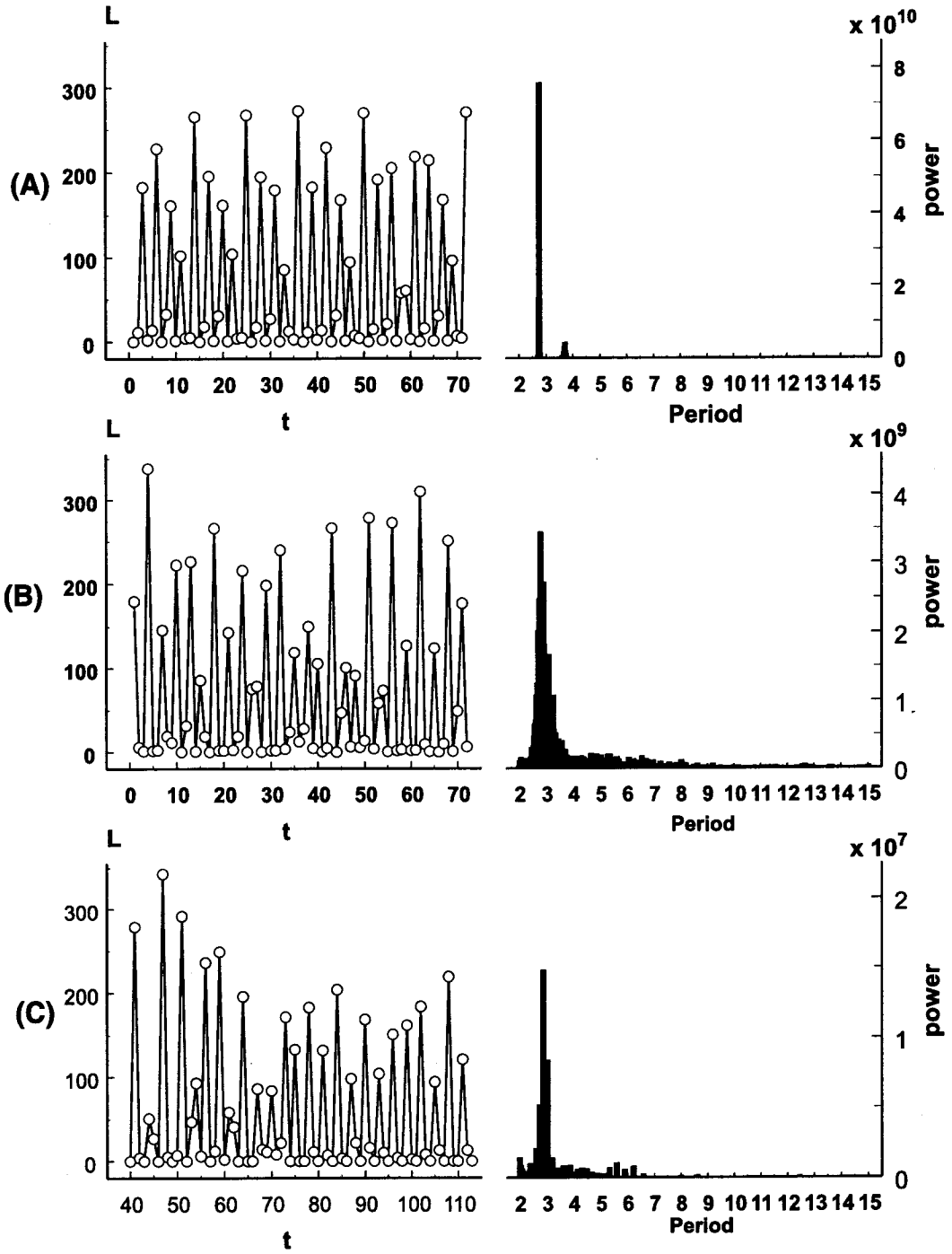

Fig. 12. Graph (A) shows the L component of an orbit on the chaotic attractor of the deterministic model (1) and its power spectrum. Graphs (B) show the same for an orbit of the demographic noise model (2). Graphs (C) show the L component of one replicate of the experimental data for treatment $c_{pa} = 0.35$ and its power spectrum.

not all, of phase space is visited with probability 1. Strictly speaking, a stochastic model cannot exhibit equilibria, periodic cycles or chaos.

Our approach to this issue is to validate a model whose deterministic skeleton can be shown, in quantifiable ways [11], to greatly influence the stationary distribution of the stochastic model and the temporal dynamics of the stochastic orbits. In this way, we conclude that the dynamics of the flour beetles

in our experiments are largely explained by known deterministic factors. It is in this sense that we mean their dynamics have deterministic properties and features, such as an equilibrium, a periodic cycle, etc. In particular, when we say the dynamics of the beetle cultures in the treatment $c_{pa} = 0.35$ are "chaotic", we mean the dynamics are largely explained by a chaotic attractor of a deterministic model.

Our approach of identifying a deterministic skeleton preserves the definition of chaos as a deterministic concept, even though our biological system is stochastic. In so doing, we avoid the confusion arising from notions that mix chaos with stochasticity (e.g. "stochastic chaos" and "noise induced chaos"). We do not rely on insufficient diagnostic tests for chaos such as a positive SLE. [5] While a positive SLE estimated from our data would provide a measure of sensitivity to initial conditions and corroborating evidence of a known chaotic attractor of a validated deterministic model, a positive SLE alone would not be sufficient to provide convincing evidence of chaos [27].

Our experiments are manipulative laboratory experiments. However, the laboratory conditions are not unlike those of "wild" populations of flour beetles growing in stored grain containers. Nor are the manipulations, resulting in high adult mortality and low adult recruitment, unrealistic perturbations; they might occur for any number of reasons (for example, a pest management strategy). Nonetheless, it remains to be investigated what implications the demonstration of chaos in a laboratory setting might have for populations in natural settings. What can be said is that we have now, for the first time, an unequivocal example of chaotic dynamics in a biological population [4,28] and that this example provides a baseline for further studies of chaos in ecology.

Acknowledgements

The research described in this paper was supported by US National Science Foundation Grants DMS-9625576 and DMS-9616205. Aaron King was supported by a post-doctoral fellowship from the Flinn Foundation under the Biology, Mathematics and Physics Initiative at the Interdisciplinary Program on Applied Mathematics, University of Arizona, Tucson.

References

[1] May RM. Biological populations with nonoverlapping generations: stable points, stable cycles and chaos. Science 1974;186:645–7.
[2] May RM. Simple mathematical models with very complicated dynamics. Nature 1976;261:459–67.
[3] Li TY, Yorke JA. Period three implies chaos. Am Math Monthly 1975;82:985–92.
[4] Zimmer C. Life after chaos. Science 1999;284:83–6.
[5] Aber JD. Why don't we believe the models?. Bull Ecol Soc Am 1997;78:232–3.
[6] Cushing JM, Costantino RF, Dennis B, Desharnais RA, Henson SM. Nonlinear population dynamics: models, experiments and data. J Theoret Biol 1998;194(1):1–9.
[7] Dennis B, Desharnais R, Cushing A, Costantino J. Nonlinear demographic dynamics: mathematical models statistical methods and biological experiments. Ecol Monogr 1995;65:261–81.
[8] Costantino RF, Cushing JM, Dennis B, Desharnais RA. Experimentally induced transitions in the dynamics behaviour of insect populations. Nature 1995;375:227–30.
[9] Dennis B, Desharnais RA, Cushing JM, Costantino RF. Transitions in population dynamics: equilibria to periodic cycles to aperiodic cycles. J Animal Ecol 1997;66:704–29.
[10] Costantino RF, Desharnais RA, Cushing JM, Dennis B. Chaotic dynamics in an insect population. Science 1997;275:389–91.
[11] Dennis B, Desharnais RA, Cushing JM, Henson SM, Costantino RF. Estimating chaos and complex dynamics in an insect population [to appear in Ecol Monogr].

[5] Even in deterministic systems a positive Lyapunov exponent is not sufficient for chaos [23]. Neither is a positive SLE sufficient for the presence of chaos in a stochastic system [27]. The stationary distribution might have sufficient weight in diverging regions of phase space, such as near repelling equilibria (or cycles) or stable manifolds of saddles, so as to cause the averaging used in the calculation of the SLE to result in a positive number. This could occur when no chaos is present in the deterministic skeleton. For example, the famous Ricker model, with a stable equilibrium, can have a positive SLE when environmental noise is added [27]. To designate a "noisy equilibrium" as "chaos" is to lose the fundamental importance of the concept of chaos, namely, that a low dimensional deterministic process can result in complicated, even random looking dynamics. A positive SLE indicates a sensitivity to initial conditions, but this sensitivity may be due to causes fundamentally different from chaos.

[12] Cushing JM, Dennis B, Desharnais RA, Costantino RF. Moving toward an unstable equilibrium: saddle nodes in population systems. J Animal Ecol 1998;67(1):298–306.
[13] Henson SM, Cushing JM, Costantino RF, Dennis B, Desharnais RA. Phase switching in population cycles. Proc R Soc 1998;265:2229–34.
[14] Henson SM, Costantino RF, Cushing JM, Dennis B, Desharnais RA. Multiple attractors saddles and population dynamics in periodic habitats. Bull Math Biol 1999;61:1121–49.
[15] Costantino RF, Cushing JM, Dennis B, Desharnais RA, Henson SM. Resonant population cycles in temporally fluctuating habitats. Bull Math Biol 1998;60(2):247–75.
[16] Henson SM, Cushing JM. The effect of periodic habitat fluctuations on a nonlinear insect population model. J Math Biol 1997;36:201–26.
[17] Park T, Mertz DB, Grodzinski W, Prus T. Cannibalistic predation in populations of flour beetles. Physiol Zool 1965;38:289–321.
[18] Cushing JM. An introduction to structured population dynamics. CBMS-NSF Regional Conference Series in Applied Mathematics 71. Philadelphia, PA: Society for Industrial and Applied Mathematics, 1998.
[19] Hale JK. Asymptotic behavior of dissipative systems. Mathematical Surveys and Monographs 25. Providence, RI: American Mathematical Society, 1985.
[20] Tong H. Nonlinear time series: a dynamical systems approach. Oxford: Oxford University Press, 1990.
[21] May RM. Stability and complexity in model ecosystems. Princeton, NJ: Princeton University Press, 1974.
[22] Shaffer ML. Minimum population sizes for species conservation. Biosci 1981;31:131–4.
[23] Alligood KT, Sauer TD, Yorke JA. Chaos: an introduction to dynamical systems. Berlin: Springer, 1997.
[24] McCaffery DF, Ellner S, Galland AR, Nychka DW. Estimating the Lyapunov exponent of a chaotic system with a nonparametric regression. J Am Statist Assoc 1992;87:682–95.
[25] King AA, Schaffer W.M. The rainbow bridge: Hamiltonian limits and resonance in predator–prey dynamics. J Math Biol 1999; 39:439–469.
[26] Beniot HP, McCauley E, Post J. Testing the demographic consequences of cannibalism in *Tribolium confusum*. Ecol 1998;79:2839–51.
[27] Desharnais RA, Costantino RF, Cushing JM, Dennis B. Estimating chaos in an insect population. Science 1997;276:1881–2.
[28] Godfray C, Hassell M. Chaotic beetles. Science 1997;275:323–4.